

Thermal Absorption/Generation on Ferro-fluid Combined Convective Flow Over Curvilinear Porous Surfaces

KH. Abdul Maleque *

Abstract- In the influence of fluid buoyancy forces, the ferrofluid combined convective flow in porous curvilinear surfaces is studied with thermal generation/absorption effect. In the ambient flow conditions, the pressure gradient terms and ferrofluid buoyancy forces are replaced by the free stream velocity $U_R = \sqrt{U_e^2 + V_e^2}$. The governing equations of the present problem are converted to ODEs by introducing non-dimensional functions and similarity variable. Boundary conditions of first derivative of velocities and temperature of our problem were constructed by the initial value problem, also the unknown initial conditions are found by shooting methods, and then a set of ODEs is solved numerically by the integration scheme of the six-order Range-Kutta method. The results of the solutions are presented graphically of velocity and thermal profiles with the help of MATLAB for different values of suction parameter P_w and heat absorption parameter β . Finally, the comparisons of the results highlight the justification of the numerical calculation accepted in the presence study. The problems in curvilinear surface study of boundary layer flow are complicated in fluid mechanics with applications of natural science and engineering.

Keywords: Curvilinear Porous surfaces, FHD flow, Combined convection, Buoyancy forces, Heat absorption/Generation.

I. Introduction

Generally, the problems in curvilinear surface study of boundary layer flow are complicated in fluid mechanics with applications of natural science and engineering. When the viscous fluid flows on the cooled (heated) inclined orthogonal surfaces, then the velocity boundary layer and thermal boundary layer are made. For significant components of the mainstream flow

$(U_e(\xi, \eta, 0), V_e(\xi, \eta, 0), 0)$ and the temperature difference $\Delta T(\xi, \eta, 0)$ between the wall and the outer fluid. A similar solution of Prandtl boundary layer flow for three-dimensional general curvilinear surfaces was studied by Hansen [1] for force flow. The different possible cases are investigated for the incompressible fluid flows in general curvilinear surfaces theoretically and numerically by Maleque [2] in his M. Phil thesis. The mixed convective boundary layer flows over curvilinear surfaces were studied theoretically by Zakerullah and Maleque [3]. They have formed the similarity requirements and detailed analysis to reduce a set of governing equations to a set of ODEs. Moreover, they have exhibited the possible various cases of ambient stream velocities, and thermal different variations for onward flow in the table. The flows in curvilinear coordinates were discussed by Cebeci et al. [4] and Blumberg et al [5]. Using an implicit finite difference method, Hung et al [6] solved the Navier-Stokes' equations on a curvilinear surface. The vector differential operator ∇ was studied by Redzic and Dragam V [7] in orthogonal curvilinear coordinates. Analysis of the flow in a curvilinear channel studied by Mario Krzyk and Matjaz Cetina [8]. They discussed mathematical models based on the rectangular coordinates system transformed to the model based on curvilinear orthogonal numerical mesh. The curvilinear coordinate was used for the flow electrically conducting fluid over a curve surfaces were discussed by Shafiq et al [9]. Recently, Kianoosh et al [10] have derived the velocity boundary and thermal boundary equations in a curvilinear system relevant to the water wave surface.

Considering, effect of thermal generation/absorption effect, Maleque [11] presented transient convective flow of MHD fluid due to a rotating disk. He solved his problems by implicit finite difference method. The activation energy, chemical reaction, and heat absorption/generation on time dependent flow past a vertical plate were discussed by Maleque[12-13]. Maleque and Siddikua [14] studied the effects of variable electro-conductivity and thermal absorption on MHD fluid heat transfer flow in vertical porous plates.

Recently, Maleque [15] has studied combined convection flow over the orthogonal curvilinear surfaces. He constructed in his paper the similarity requirements of ambient velocities and temperature difference for various conditions of the flow that transform the PDEs to ODEs.

Kh. Abdul Maleque
American International University-Bangladesh,
Kuratali, Dhaka-1219, Bangladesh, email:
maleque@aiub.edu,
<https://orcid.org/0000-0001-6649-7580>

Along with the above works, we consider the non-Newtonian Ferro hydrodynamic (FHD) fluid flow in our present paper. With the influence of buoyancy forces, we consider the results of heat generation and absorption on combined convection flow of ferrofluid fluid over vertical porous curvilinear surfaces. It is concerned to convert the simultaneous PDEs for mixed convection laminar flow of incompressible fluid in curvilinear surfaces to simultaneous ODEs by using non-dimensional functions and variables. After that by applying six ordered Runge-Kutta integration schemes and shooting method, we solved the set of ordinary differential equations numerically and the results are shown graphically as the profiles of primary and secondary velocity, and temperature. We also displayed the tabular form of calculating results of skin friction of both primary and secondary and the rate of heat transfer by taking various values of different parameters that are our physical interest. The problems in curvilinear surface study of boundary layer flow are complicated in fluid mechanics with applications of natural science and engineering. A uniform flow at the entrance to a pipe, a motor car and a aero foil etc. The investigation of boundary-layer flows over aerodynamic surfaces is our problem of major importance.

II. Geometrical representation of the flow

In our present study, the heated inclined vertical orthogonal curvilinear surfaces are considered. The free stream velocity $(U_e(\xi, \eta), V_e(\xi, \eta), 0)$ normal to ζ -axis shown in Fig.1 (Maleque [2], Zakerullah et al [3]). Due to the buoyancy effects of the fluid, acceleration vector $\vec{g}(-g_\xi(\xi, \eta), -g_\eta(\xi, \eta), 0)$ in the direction ξ – and η to heated surface. Considering orthogonal curvilinear coordinates and the idea of Prandtl flow the governing equations are.

$$\frac{\partial}{\partial \xi}(h_2 u) + \frac{\partial}{\partial \eta}(h_1 v) + \frac{\partial}{\partial \zeta}(h_1 h_2 w) = 0, \quad (1)$$

$$\rho \left(\frac{u}{h_1} \frac{\partial u}{\partial \xi} + \frac{v}{h_2} \frac{\partial u}{\partial \eta} + w \frac{\partial u}{\partial \zeta} + \frac{uv}{h_1 h_2} \frac{\partial h_1}{\partial \eta} - \frac{v^2}{h_1 h_2} \frac{\partial h_2}{\partial \xi} \right) = -\frac{1}{h_1} \frac{\partial p}{\partial \xi} + \rho g_\xi \beta_T (T - T_e) + \frac{\sigma_0 M_a \partial H}{h_1} \frac{\partial H}{\partial \xi} + \mu \frac{\partial^2 u}{\partial \zeta^2} \quad (2)$$

$$\rho \left(\frac{u}{h_1} \frac{\partial v}{\partial \xi} + \frac{v}{h_2} \frac{\partial v}{\partial \eta} + w \frac{\partial v}{\partial \zeta} + \frac{uv}{h_1 h_2} \frac{\partial h_2}{\partial \xi} - \frac{u^2}{h_1 h_2} \frac{\partial h_1}{\partial \eta} \right) = -\frac{1}{h_2} \frac{\partial p}{\partial \eta} + \rho g_\eta \beta_T (T - T_e) + \frac{\sigma_0 M_a \partial H}{h_2} \frac{\partial H}{\partial \eta} + \mu \frac{\partial^2 v}{\partial \zeta^2} \quad (3)$$

$$\frac{\partial p}{\partial \zeta} = 0, \quad (4)$$

$$\rho C_p \left(\frac{u}{h_1} \frac{\partial T}{\partial \xi} + \frac{v}{h_2} \frac{\partial T}{\partial \eta} + w \frac{\partial T}{\partial \zeta} \right) = k \frac{\partial^2 T}{\partial \zeta^2} + Q_0 (T - T_e). \quad (5)$$

Subject to the boundary conditions of the flow field as the velocities and temperature are:

$$\left. \begin{aligned} u = 0, v = 0, w = w_0(\xi, \eta, 0), T = T_w, \text{ at } \zeta = 0 \\ u \rightarrow U_e, v \rightarrow V_e, T \rightarrow T_e \text{ as } \zeta \rightarrow \infty \end{aligned} \right\} \quad (6)$$

w_0 represents the suction ($w_0 > 0$) / injection ($w_0 < 0$) velocity for the developable surface at $\zeta = 0$.

Considering $\rho = \rho(P, T)$. For Boussinesq fluid approximation $\beta_T = -\frac{1}{\rho} \left(\frac{\partial \rho}{\partial T} \right)_p$ has substituted in the

above equations where $\beta_T = -\frac{1}{\rho} \left(\frac{\partial \rho}{\partial T} \right)_p$ be the thermal expansion coefficient for the fluid, specific heat C_p with constant pressure and the heat generation (> 0) or absorption (< 0) coefficient Q_0 , σ_0 is the magnetic permeability and μ be fluid viscosity, and \vec{B} is vector magnetic induction. Here $h_3(\xi, \eta) = 1$ is considered such that ζ denotes the original distance calculated perpendicular to the surface. For ambient flow, the free stream potential flow $(U_e(\xi, \eta), V_e(\xi, \eta), 0)$ and the ambient temperature T_e are the functions of (ξ, η) . Therefore, component of free stream velocity U_e and V_e and ambient temperature T_e do not depend on ζ .

Imposing the outer flow conditions $u \rightarrow U_e, v \rightarrow V_e, \rho \rightarrow \rho_e, T \rightarrow T_e (= \text{constant}), \frac{\partial}{\partial \zeta} \rightarrow 0$, we eliminate

the pressure terms $\frac{\partial p}{\partial \xi}$ and $\frac{\partial p}{\partial \eta}$ and Ferro fluid terms $\frac{\sigma_0 M_a \partial H}{h_1} \frac{\partial H}{\partial \xi}$ and $\frac{\sigma_0 M_a \partial H}{h_2} \frac{\partial H}{\partial \eta}$ from equations (2) and (3). The following equations are found:

$$\rho_e \left(\frac{U_e}{h_1} \frac{\partial U_e}{\partial \xi} + \frac{V_e}{h_2} \frac{\partial U_e}{\partial \eta} + \frac{U_e V_e}{h_1 h_2} \frac{\partial h_1}{\partial \eta} - \frac{V_e^2}{h_1 h_2} \frac{\partial h_2}{\partial \xi} \right) = -\frac{1}{h_1} \frac{\partial p}{\partial \xi} + \frac{\sigma_0 M_a \partial H}{h_1} \frac{\partial H}{\partial \xi} \quad (7)$$

$$\rho_e \left(\frac{U_e}{h_1} \frac{\partial V_e}{\partial \xi} + \frac{V_e}{h_2} \frac{\partial V_e}{\partial \eta} + \frac{U_e V_e}{h_1 h_2} \frac{\partial h_2}{\partial \xi} - \frac{U_e^2}{h_1 h_2} \frac{\partial h_1}{\partial \eta} \right) = -\frac{1}{h_2} \frac{\partial p}{\partial \eta} + \frac{\sigma_0 M_a \partial H}{h_2} \frac{\partial H}{\partial \eta} \quad (8)$$

$$\rho_e \left(\frac{U_e}{h_1} \frac{\partial T_e}{\partial \xi} + \frac{V_e}{h_2} \frac{\partial T_e}{\partial \eta} \right) = 0. \quad (9)$$

The solution of equation (9) is the form $T_e = T_0 (= \text{constant})$.

After elimination of the pressure terms [equations (7) and (8)], the momentum and energy equations take the form:

$$\frac{\partial}{\partial \xi}(h_2 u) + \frac{\partial}{\partial \eta}(h_1 v) + \frac{\partial}{\partial \zeta}(h_1 h_2 w) = 0, \quad (10)$$

$$\begin{aligned} \frac{u}{h_1} \frac{\partial u}{\partial \xi} + \frac{v}{h_2} \frac{\partial u}{\partial \eta} + w \frac{\partial u}{\partial \zeta} + \frac{uv}{h_1 h_2} \frac{\partial h_1}{\partial \eta} - \frac{v^2}{h_1 h_2} \frac{\partial h_2}{\partial \xi} \\ = g_\xi \beta_T (T - T_0) + v \frac{\partial^2 u}{\partial \zeta^2} + \frac{U_e \partial U_e}{h_1} \frac{\partial U_e}{\partial \xi} \\ + \frac{V_e \partial U_e}{h_2} \frac{\partial U_e}{\partial \eta} + \frac{U_e V_e \partial h_1}{h_1 h_2} \frac{\partial h_1}{\partial \eta} - \frac{V_e^2 \partial h_2}{h_1 h_2} \frac{\partial h_2}{\partial \xi} \end{aligned} \quad (11)$$

$$\begin{aligned} \frac{u}{h_1} \frac{\partial v}{\partial \xi} + \frac{v}{h_2} \frac{\partial v}{\partial \eta} + w \frac{\partial v}{\partial \zeta} + \frac{uv}{h_1 h_2} \frac{\partial h_2}{\partial \xi} - \frac{u^2}{h_1 h_2} \frac{\partial h_1}{\partial \eta} \\ = g_\eta \beta_T (T - T_0) + v \frac{\partial^2 v}{\partial \zeta^2} + \frac{U_e \partial V_e}{h_1} \frac{\partial V_e}{\partial \xi} + \frac{V_e \partial V_e}{h_2} \frac{\partial V_e}{\partial \eta} \\ + \frac{U_e V_e \partial h_2}{h_1 h_2} \frac{\partial h_2}{\partial \xi} - \frac{U_e^2 \partial h_1}{h_1 h_2} \frac{\partial h_1}{\partial \eta}, \end{aligned} \quad (12)$$

$$\rho C_p \left(\frac{u}{h_1} \frac{\partial T}{\partial \xi} + \frac{v}{h_2} \frac{\partial T}{\partial \eta} + w \frac{\partial T}{\partial \zeta} \right) = k \frac{\partial^2 T}{\partial \zeta^2} + Q_0 (T - T_0) \quad (13)$$

III. Similarity Transformations

Recently, Maleque [15] has derived the possible cases of similarity solutions and found the nature of free stream velocity components (U_e, V_e) and Gabriel lame coefficients (h_1, h_2) and ΔT -variations for which transform the PDEs (10)-(13) to a set of nonlinear ODEs. The present investigation concerns one of the possible similarity solutions. In this paper, we consider the physical variables as the following dimensionless functions (similarity) and dimensionless variable (similarity):

$$U_e = U_0 (a \xi + b \eta)^m, \quad h_1 = (a \xi + b \eta)^n, \quad V_e = k_1 U_e, \quad h_2 = k_2 h_1, \quad \Delta T = (\Delta T)_0 (a \xi + b \eta)^{2m-n-1},$$

$$u = U_e f_\phi(\phi), \quad v = V_e g_\phi(\phi), \quad T - T_0 = \Delta T \vartheta(\phi),$$

$$T_w - T_0 = \Delta T(\xi, \eta) \quad \text{and}$$

$$\phi = \zeta \left[\frac{a(3n+m+1)U_0}{2\nu} \right]^{\frac{1}{2}} (a\xi + b\eta)^{\frac{m-n-1}{2}}.$$

Introducing the above similarity functions and variables in equations (10)–(13). The momentum equations (11-12) and energy equation (13) take the same forms

$$f_{\phi\phi\phi} + (f + cg)f_{\phi\phi} + \left(\frac{2m}{3n+m+1} \right) (1 - f_\phi^2) + 2c \left(\frac{m+n}{3n+m+1} \right) (1 - f_\phi g_\phi) + P_w f_{\phi\phi} - \left(\frac{2nc}{3n+m+1} \right) (1 - g_\phi^2) + \frac{U_F^2}{U_e^2} \vartheta = 0, \quad (14)$$

$$g_{\phi\phi\phi} + (f + cg)g_{\phi\phi} + \left(\frac{2mc}{3n+m+1} \right) (1 - g_\phi^2) + 2 \left(\frac{m+n}{3n+m+1} \right) (1 - f_\phi g_\phi) + P_w g_{\phi\phi} - 2 \left(\frac{n}{3n+m+1} \right) (1 - f_\phi^2) + \frac{V_F^2}{V_e^2} \vartheta = 0, \quad (15)$$

$$P_r^{-1} \vartheta_{\phi\phi} + (f + cg)\vartheta_\phi + P_w \vartheta_\phi - 2 \left(\frac{2m-n-1}{3n+m+1} \right) (f_\phi + cg_\phi)\vartheta + \beta \vartheta = 0. \quad (16)$$

Here, the fluid buoyancy forces are

$$U_F^2 = g_\xi \beta_T \Delta T \times \text{characteristic length},$$

$$V_F^2 = g_\eta \beta_T \Delta T \times \text{characteristic length},$$

$$\text{and characteristic length} = \frac{a\xi + b\eta}{a(3n+m+1)}.$$

Equation (6) is transformed to non-dimensional form,

$$\left. \begin{aligned} f(0) &= P_w - cg(0), \quad f_\phi(0) = 0, \quad f_\phi(\infty) = 1, \\ g(0) &= g_0, \quad g_\phi(0) = 0, \quad g_\phi(\infty) = 1, \\ \vartheta(0) &= 1, \quad \vartheta(\infty) = 0. \end{aligned} \right\} \quad (17)$$

The solution of equation (10) w -velocity which is normal to the surface is found to be

$$w = \left(\frac{\nu a U_0}{2} \right)^{\frac{1}{2}} \left(\frac{3n+m+1}{2} \right)^{\frac{1}{2}} (a\xi + b\eta)^{\frac{m-n-1}{2}} \times \left[f + cg - \varphi \left(\frac{n+1-m}{3n+m+1} \right) (f_\phi + cg_\phi) \right], \quad (18)$$

where

$$P_w = w_w \left(\frac{\nu a U_0}{2} \right)^{-\frac{1}{2}} \left(\frac{3n+m+1}{2} \right)^{-\frac{1}{2}} (a\xi + b\eta)^{\frac{n+1-m}{2}},$$

$$c = \frac{k_1 b}{k_2 a}, \quad P_r = \frac{\rho \nu C_p}{k}, \quad \beta = \frac{Q_0 h_1 (a\xi + b\eta)}{a(3n+m+1)\rho C_p U_e}.$$

The irrotational condition for mainstream flow is $(h_2 V_e)_\xi - (h_1 U_e)_\eta = 0$, which yields $m = -n$ or $c = k_1^2$, here $m \neq -n$ is considered.

Under the boundary conditions (eq17), equation (18) and applying Nachtsheim-Swigert [16] iteration technique with RK-6 integration scheme, we solve the eq(14)-eq(16) numerically and display the results graphically and tabular form.

IV. Comparison

Well known Falkner-Skan equation is found by considering $U_F = V_F = 0, c = 0, n = 0$, and $P_w = 0$ in the above equations (14-16) in the absence of heat generation and buoyancy force. It shows the great agreement with the present work and the Falkner Skin solution, and it also shows the validity of our numerical solution. Moreover If $A = 0, c = 0, k_1 = 0, U_F = 0, \beta = 0$ and $P_w = 0$ equation(14) coincides with the equation of Sparrow et. al [17].

V. Solution

Numerical solutions of equations (17)–(20) are found by applying RK-6 integration scheme with Nachtsheim-Swigert [23] iteration technique. For different values of buoyancy parameters $\frac{U_F^2}{U_e^2}$, and $\frac{V_F^2}{V_e^2}$, suction/injection parameter P_w , Prandtl number P_r , and exponents m, n, c , numerical results are calculated. From the numerical calculation, $f_\phi(0), g_\phi(0)$ and $\vartheta(0)$ are found, which are our required physical interests, that is, the shear stresses (τ_u, τ_v) and the rate of heat transfer q_w . To find the primary and secondary shear stresses (τ_u, τ_v) and the thermal transfer rate q_w , applying the following Newtonian formulae

$$\tau_u = \mu \left(\frac{\partial u}{\partial \zeta} + \frac{1}{h_1} \frac{\partial w}{\partial \xi} \right)_{\zeta=0},$$

$$\tau_v = \mu \left(\frac{\partial v}{\partial \zeta} + \frac{1}{h_2} \frac{\partial w}{\partial \eta} \right)_{\zeta=0},$$

$$\text{and } q_w = -k \left(\frac{\partial T}{\partial \zeta} \right)_{\zeta=0}.$$

Primary skin friction

$$S_{ku} = \frac{\tau_u}{\frac{1}{2}\rho U_e^2} = R_{eu}^{-\frac{1}{2}} \left[\frac{3n+m+1}{h_1(a\xi+b\eta)} \right]^{\frac{1}{2}} f_{\phi\phi}(0),$$

Secondary skin friction

$$S_{kv} = \frac{\tau_v}{\frac{1}{2}\rho V_e^2} = R_{ev}^{-\frac{1}{2}} \left[\frac{3n+m+1}{ch_2(a\xi+b\eta)} \right]^{\frac{1}{2}} g_{\phi\phi}(0),$$

and the Nusselt number

$$N_u = \frac{q_w}{ak\Delta T} = -R_{eu}^{\frac{1}{2}} \left[\frac{3n+m+1}{2h_1(a\xi+b\eta)} \right]^{\frac{1}{2}} \vartheta_{\phi}(0),$$

where $R_{eu} = \frac{U_e}{\nu}$, and $R_{ev} = \frac{V_e}{\nu}$ are primary and secondary Reynold numbers respectively. Noted that

$\left[\frac{3n+m+1}{h_1(a\xi+b\eta)} \right]^{\frac{1}{2}}$, and $\left[\frac{3n+m+1}{ch_2(a\xi+b\eta)} \right]^{\frac{1}{2}}$ both are dimensionless quantities where as a and b both have dimension (meter⁻¹). The numerical solutions are presented as primary velocity and secondary velocity as u, v velocities respectively, and the temperature profiles, are presented graphically and the corresponding primary and secondary shear stresses and Nusselt number are displayed in the table.

VI. Results and Discussions

We present the numerical solution as primary (u) velocity, secondary (v) velocity profiles, and temperature (T) profiles for effects of different parameters $\frac{U_F^2}{U_e^2}, \frac{V_F^2}{V_e^2}, P_w, P_r, m, n,$ and c . We obtained the numerical results with the effects of various values of one parameter and the others are keeping constants.

6.1 Heat absorption/generation (β) effects:

The continuity and momentum equations have no effect directly on heat generation\absorption. The effect comes through the temperature equation that means buoyancy force. It has been found from Fig.2, dimensionless coefficient of thermal generation and absorption (β) has remarkable effects on primary/secondary velocities and temperature profiles in the presence of buoyancy forces. Considering $\beta = -1, 0, +1$ for heat absorption and generation, respectively. $\beta = 0$ represents the heat absorption/generation has no effect on velocity and temperature boundary layer. Fig2. shows that absorption coefficient is to contract the velocity boundary layer and thermal boundary layer thickness. That is, both u -velocity (f_{ϕ}), v -velocity (g_{ϕ}) profile as well as T -temperature profile (ϑ_{ϕ}) decrease with

decreasing values of thermal absorption coefficient ($\beta < 0$). Opposite effects are found for the heat generation effect ($\beta > 0$). The thickness of heat boundary layer thickness increases with the increase of thermal generation. It also has been observed from Fig.2, the coefficient of thermal generation is to increase the velocities and temperature profiles.

Table-1 shows that the dimensionless coefficient of thermal absorption/generation has remarkable results on shearing stresses and heat transfer rate. The coefficient of heat absorption effects are to contract temperature boundary layer. The primary as well as secondary skin friction coefficients, and heat flux increase with coefficient of thermal absorption/generation increase. Therefore, more energy is supplied through the surface to keep the constant temperature of the surface for increasing the value of heat absorption coefficient, that is, the heat flux increases.

6.2 Effects of porous parameter (P_w):

Fig.3 and Fig.4 show the effects of porous parameter P_w on u -velocity, v -velocity, and temperature. In the Fig.3, we consider the different values $P_w = -0.5, 0, 0.5$ for fixed values primary buoyancy force $\frac{U_F^2}{U_e^2} = 50$ and secondary buoyancy force $\frac{V_F^2}{V_e^2} = 1$. $P_w < 0$, $P_w > 0$, and $P_w = 0$ represent the injection, suction and no suction/injection, respectively.

Primary velocity & temperature profiles decrease, and secondary velocity increases for increase of the suction parameter P_w shown in Fig.3. That is, primary and temperature boundary layer thickness are reduced by increasing values of P_w for a large values of primary buoyancy force $\frac{U_F^2}{U_e^2} = 50$. On the contrary, we consider the different values $P_w = -1, 0, 1$ for fixed values primary buoyancy force $\frac{U_F^2}{U_e^2} = 1$ and secondary buoyancy force $\frac{V_F^2}{V_e^2} = 50$ as shown in the Fig.4. We observed from Fig-4. that the opposite effects are found in primary and secondary velocities for a large values of secondary buoyancy force $\frac{V_F^2}{V_e^2} = 50$ also similar effects are found for temperature profiles.

Increase of P_w leads to secondary v -velocity and temperature profiles decrease, and primary velocity profile increases. Therefore, secondary and temperature thicknesses are reduced by the increasing values of P_w for large value of secondary buoyancy force $\frac{V_F^2}{V_e^2} = 50$ shown in Fig.4.

Table-2 shows influence of buoyancy parameters $\frac{U_F^2}{U_e^2} = 10, \frac{V_F^2}{V_e^2} = 5$, the effect of the coefficients of shearing stresses and heat flux for changing values of suction/injection P_w .

References

- [1] Hansen, A. G., "Possible similarity solution of the laminar incompressible boundary layer equations", ASME paper 57 A, 79, 1957.
- [2] Maleque Kh. A., "Similarity solutions of combined forced and free convective laminar boundary layer flows in curvilinear coordinates", M. Phil thesis, Dept. of Math, Central library of BUET, 1995.
- [3] Zakerullah Md., and Maleque, Kh. A., "Similarity requirements for combined forced and free convective laminar boundary layer flow over vertical curvilinear surfaces", J. Bangladesh academy of sciences, Vol-22(1), pp 79-90, 1998.
- [4] Cebeci, T., Kaups, K., and Moser, A., "Calculation of three-dimensional boundary AIAA journal 14(8), 1090-1094, 1976.
- [5] Blumberg, A. F., and Herring, H. J., "Circulation modelling using orthogonal curvilinear coordinates", In Elsevier oceanography series, vol-45, pp. 55-88, 1987.
- [6] Hung, T. K., and Brown, T. D., "An implicit finite-difference method for solving the navier-stokes equation using orthogonal curvilinear coordinates", Journal of Computational Physics, Vol 23(4), 343-363, 1977.
- [7] Redzic, Dragan V., "The operation ∇ in orthogonal curvilinear coordinates", European Journal of Physics, vol 22(6), 595, 2001.
- [8] Mario Krzyk, and Matjaz Cetina, "Analysis of flow in a curved channel using the curvilinear orthogonal numerical mesh", Journal of Mechanical Engineering,
- [9] Shafiq, A., Nadeem, S., and Nurmuhammad, "Boundary layer flow over a curve surface imbedded in porous medium", Communications in theoretical physics, Vol-71, pp-344, 2019.
- [10] Kianoosh, Youseki and Fabrice Veron, "Boundary layer formulations in orthogonal curvilinear coordinates for flow over wind generated surface waves", Journal of Fluid Mechanics, Vol-888, A11, 2020.
- [11] Maleque, Kh. A., and Sattar, M. A., "Transient convective flow due to a rotating disc with magnetic field and heat absorption effects." Journal of energy, heat and mass transfer. Vol-25, pp-279-291, 2003
- [12] Maleque, Kh. A., "Effects of Binary Chemical Reaction and Activation Energy on MHD Boundary Layer Heat and Mass Transfer Flow with Viscous Dissipation and Heat Generation/Absorption." International Scholarly Research Notices, Hindawi Publishing Corporation ISRN Thermodynamics Volume 2013, Article ID 284637, 9 pages <http://dx.doi.org/10.1155/2013/284637>.
- [13] Maleque Kh. A. "A Binary Chemical Reaction on Unsteady Free Convective Boundary Layer Heat and Mass Transfer Flow with Arrhenius Activation Energy and Heat Generation/Absorption, The Latin American Applied Research Journal (LAAR), Argentina, Vol -44, No. 1, pp- 97-104, 2014. ISSN: 0327-0793.
- [14] Maleque Kh. A., Siddikua, A., "Effect of Variable Electro-conductivity on MHD Convective Heat Transfer Flow Past A Continuous Moving Semi-Infinite Vertical Porous Plate with Heat Absorption", The AIUB Journal of Science and Engineering (AJSE), Vol-13, No. 1, pp 77-83, August 2014, ISSN 1608-3679.
- [15] Maleque, Kh. A., "Similarity requirements for mixed convective boundary layer flow over vertical curvilinear porous surfaces with heat generation/absorption", International Journal of Aerospace Engineering, March 03, 2020.
- [16] Nachtsheim, P. R., and Swigert, P., "Satisfaction of asymptotic boundary conditions in numerical solution of system of nonlinear of boundary layer type", NASA TN-D3004, 1965.
- [17] Sparrow, E. M., Eichorn, R., and Gregg, L. J., "Combined forced and free convection in a boundary layer flow", Phys. Fluids, Vol-2, pp-319, 1959.

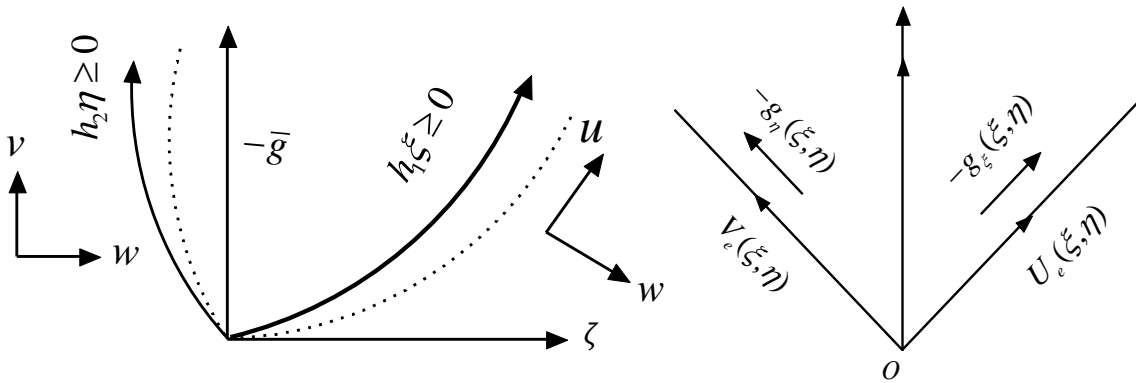


Fig.1 The geometrical representation of flow in the curvilinear coordinates

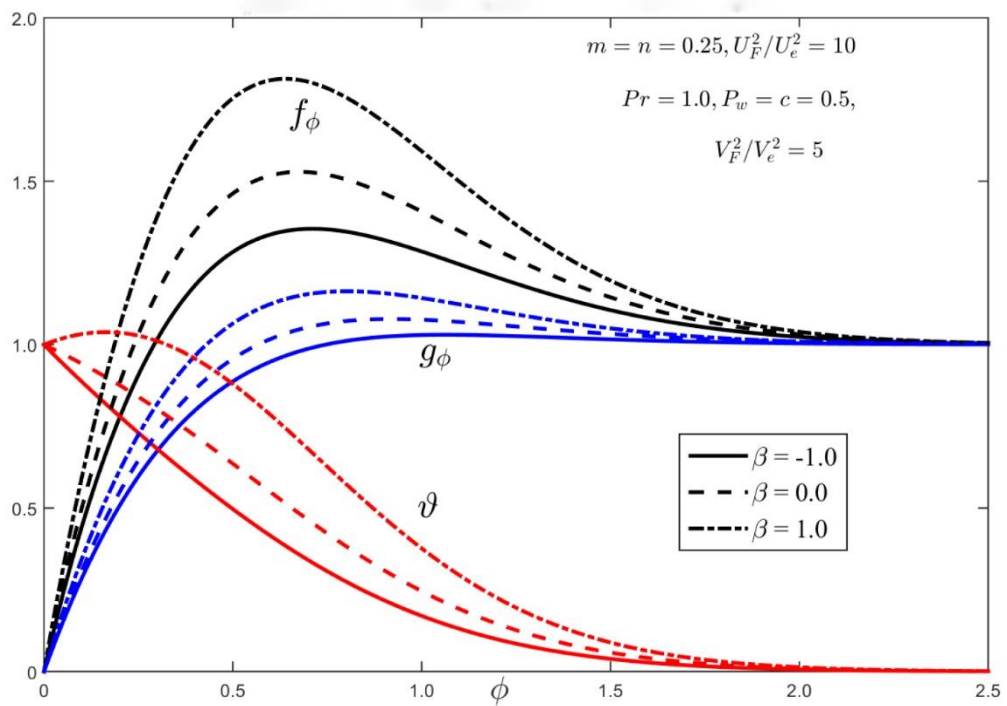


Fig.2 Effects of β on the velocities and temperature profiles

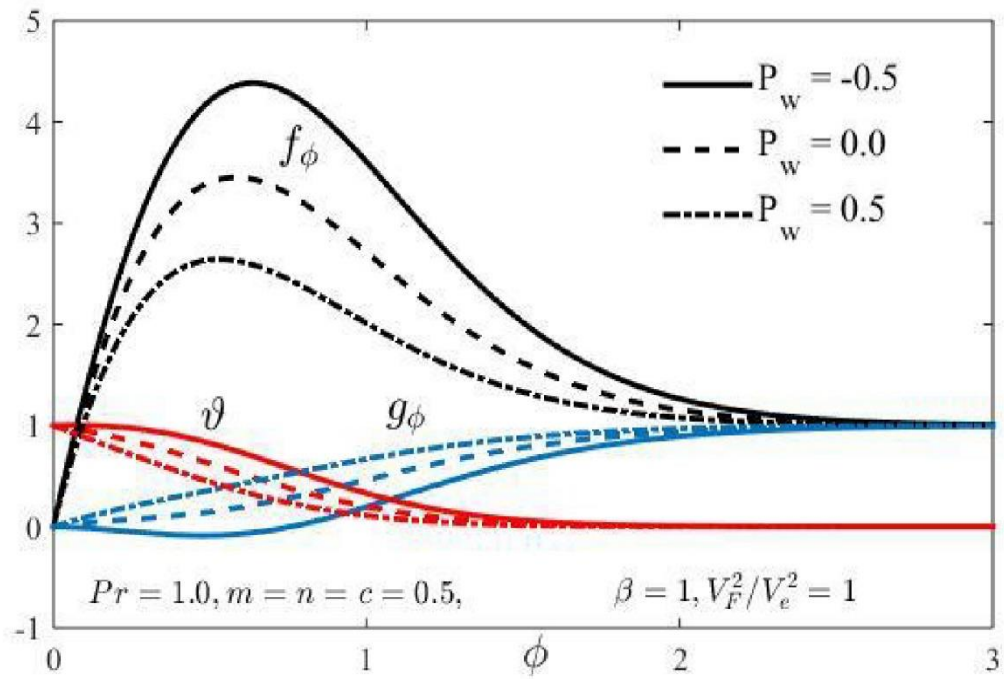


Fig.3 Effects of P_w on the velocities and temperature profiles for $\frac{U_F^2}{U_e^2} = 50$.

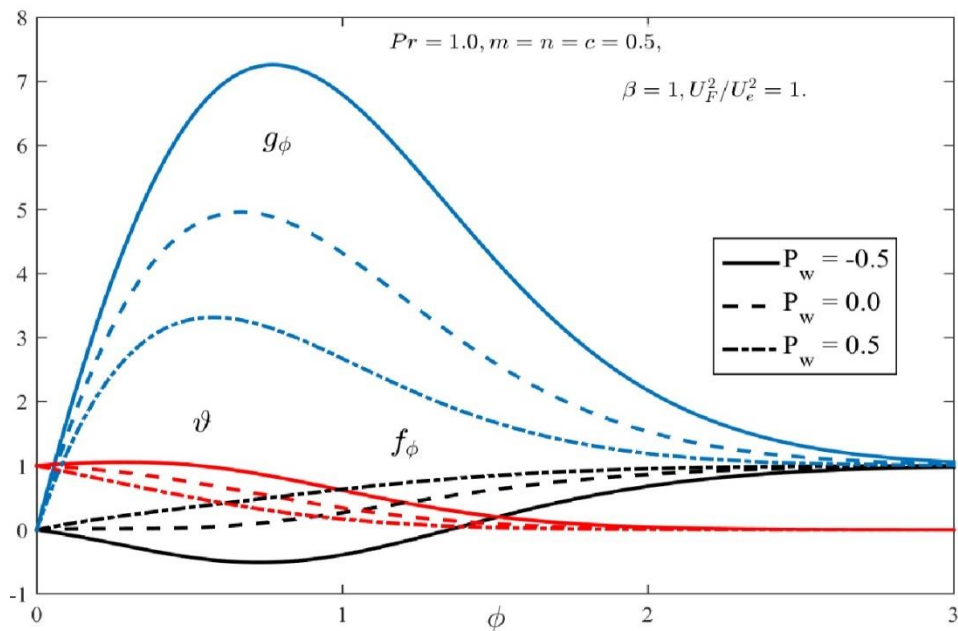


Fig.4 Effects of P_w on the velocities and temperature profiles for $\frac{V_F^2}{V_e^2} = 50$.

Table1

Effects of thermal generation/absorption (β) on shearing stresses and heat flux for $m = n = c = 0.5, \frac{U_F^2}{U_e^2} = 10, \frac{V_F^2}{V_e^2} = 5, P_w = 0.5, P_r = 1.0$

β	$f_{\phi\phi}(0)$	$g_{\phi\phi}(0)$	$\vartheta_{\phi}(0)$
-10.0	3.9047440	2.9379085	-3.5887761
-5.0	4.3599440	3.1165470	-2.7612212
-1.0	5.1011856	3.3908456	-1.7759053
0.0	5.4284228	3.5073780	-1.4191172
1.0	5.8843796	3.6644078	-0.9634404
5.0	5.4326819	3.8447401	0.3466724
10.0	6.4542250	4.2838729	3.2508243

Table-2

Effects of porous parameter P_w on shearing stresses & Nusselt number for $m = n = c = 0.5, \frac{U_F^2}{U_e^2} = 10, \frac{V_F^2}{V_e^2} = 5, P_w = 0.5, P_r = 1.0$

P_w	$f_{\phi\phi}(0)$	$g_{\phi\phi}(0)$	$\vartheta_{\phi}(0)$
-1.5	3.8584706	1.8588955	0.3406180
-1.0	4.7447542	2.2418202	0.3133609
-0.5	5.3794661	2.6682846	0.0526941
0.0	5.6306103	3.1178411	-0.4729934
0.5	5.6336459	3.5797204	-1.2081323
1.0	5.6542946	4.0721958	-2.0607794
1.5	5.8417006	4.6301253	-2.9628524